Determination of Pore Size in Mesoporous Thin Films from the Annihilation Lifetime of Positronium

T. L. Dull, W. E. Frieze, and D. W. Gidley*

Department of Physics, University of Michigan, Ann Arbor, Michigan 48109

J. N. Sun and A. F. Yee

Department of Materials Science and Engineering, University of Michigan, Ann Arbor, Michigan 48109

Received: November 14, 2000; In Final Form: February 15, 2001

An existing model that relates the annihilation lifetime of positronium trapped in subnanometer pores to the average size of the pores is extended to account for positronium in any size pore and at any temperature. This extension enables the use of positronium annihilation lifetime spectroscopy in characterizing nanoporous and mesoporous materials, in particular thin insulating films where the introduction of porosity is crucial to achieving a low dielectric constant, *K*. Detailed results of the model calculations are presented along with extensive experimental results to systematically check the lifetime vs pore size calibration in a variety of low-*K* materials over a wide range of pore sizes.

I. Introduction

Positronium annihilation lifetime spectroscopy (PALS) has long been used to study open volume regions in insulating materials such as polymers and other molecular solids. In the solid regions of such materials, the binding energy of positronium (Ps, the bound state of an electron and a positron) is reduced by a factor proportional to the dielectric constant, so that Ps preferentially localizes in regions of open volume. *para*-Positronium (*p*-Ps, the singlet spin state) has a short self-annihilation "vacuum" lifetime ($\tau = 0.125$ ns) that is not significantly perturbed by additional annihilation with molecular electrons in the solid. *ortho*-Positronium (*o*-Ps, the triplet spin state), however, lives long enough so that it can trap in voids where the triplet vacuum lifetime ($\tau = 142$ ns) can be markedly reduced by interaction with molecular electrons. This provides the physical basis for probing void volume with PALS. Ps trapped in smaller pores will have shorter lifetimes than in larger pores where τ should asymptotically approach the vacuum value. In most circumstances, it is possible to extract pore size information from PALS spectra by using a model to relate τ to pore size.

Recently much attention has been focused on developing porous materials as low-dielectric thin films for use in the next generation of microelectronics.[1] As integrated devices become smaller, the *RC*-delay time of signal propagation along interconnects becomes the dominant factor limiting overall chip speed. With the advent of copper technology, *R* has been pushed to a practical lowest limit so attention must be focused on reducing *C*. One way of accomplishing this task is to reduce the average dielectric constant *K* of the thin insulating films surrounding interconnects through the introduction of porosity. Size scales of pores in such low-*K* films typically range from 2 to 20 nm. There are few probes capable of characterizing such porosity in thin, submicron films,[2] especially when the pores are closed and inaccessible to gas absorption techniques. By using a beam of several keV positrons, however, it is possible to form Ps throughout these thin films and perform PALS.[3−7] To extract pore dimensions from such an analysis, a broadly applicable model relating Ps lifetime and pore size is required. In this paper, we will generalize an existing model that is presently restricted to Ps in subnanometer pores. We extend it to include Ps in pores of any size at any temperature. Results of these model calculations are presented, and a direct comparison with experimental Ps lifetime calibration data is provided.

II. Ps Lifetimes in Small Pores

For very small ($R < 1$ nm) pores, such as those encountered in bulk polymers, the standard of PALS calibration has been the Tao−Eldrup (TE) model.[8,9] For all of its simplicity, it has been remarkably successful relating lifetime to pore size.[10] The TE model treats the *o*-Ps atom in the pore as a single scalar particle with twice the electron mass trapped in the ground state of an infinite *spherical* potential well. In the central portion of the well, the *o*-Ps atom is assumed to have an infinite lifetime (the finite 142 ns vacuum lifetime is quite reasonably ignored), and within a distance ΔR of the walls of the potential well, the *o*-Ps atom is assumed to have the spin-averaged Ps lifetime (0.5 ns). The overall annihilation rate ($\lambda = 1/\tau$) is calculated by averaging the annihilation rate over the volume of the pore using the square of the *o*-Ps wave function as a weighting factor. Because λ_T (self-annihilation) is ignored, the calculated annihilation rate is actually the "pick-off" quenching annihilation rate because of interactions with electrons in the walls of the well/pore. Using this TE model, the annihilation rate of *o*-Ps trapped in a pore of radius $R + \Delta R$ is given by

$$\lambda_{TE}(R) = \lambda_A\left[1 - \frac{R}{R+\Delta R} + \frac{1}{2\pi}\sin\left(\frac{2\pi R}{R+\Delta R}\right)\right]$$

where $\lambda_A = (\lambda_S + 3\lambda_T)/4$ is the spin-averaged vacuum annihilation rate and λ_S and λ_T are the singlet and triplet vacuum

* To whom correspondence should be addressed. Tel: (734) 763-3464. Fax: (734) 764-5153. E-mail: gidley@umich.edu.

10.1021/jp004182v CCC: $20.00
Published on Web 04/28/2001

annihilation rates. The lifetime is $\tau_{TE}(R) = 1/\lambda_{TE}(R)$. This model has one free parameter, ΔR, which is empirically determined[11] to be 0.16−0.17 nm by fitting to data acquired in a variety of well-characterized, small-pore materials such as zeolites.

The TE treatment neglects the 142 ns *o*-Ps lifetime in the central portion of the well, and this is reasonable given the pick-off shortened 2 ns lifetime typically observed in small pores. It is trivial to add this effect to the TE model. More importantly, the model also neglects the possibility that excited states of the particle in the well may be populated. This is also reasonable because the energy gap between the ground state and the first excited state, of order 100−200 meV, is large compared to thermal energy *kT*. Alternatively, one can note that the de Broglie wavelength of thermal, room-temperature Ps is about 6 nm, 1 order of magnitude larger than the subnanometer pore size, and hence, the ground-state zero-point energy is large compared to *kT*. Improvements in the TE model focus on this feature.

III. Ps Lifetimes in Large Pores

Pore sizes in the range of 2−20 nm in diameter (or larger), such as those typically found in low-*K* films, are too large for the TE treatment to be applicable. Several attempts have been made to develop a model relating *o*-Ps lifetime to pore size for larger pores. One group has attempted to directly extend the TE model by including excited states in the calculation.[12] Although fundamentally sound, this approach fails in practice only because it becomes prohibitively cumbersome to calculate all of the necessary high order Bessel functions and their zeros required for an accurate result.[12] Even though the population of each energy state falls off exponentially, the increasing degeneracy requires that many terms be included in the sums. This difficulty, which is a consequence of the assumed *spherical* (or cylindrical) pore geometry, can be avoided by switching to *rectangular* pore geometry,[5] as will be discussed below.

In a separate attempt to calibrate Ps lifetimes in large pores, a group from the University of Tokyo has developed a semiphenomenological model to relate *o*-Ps lifetime to pore size in spherical pores of radius $R + \Delta R$.[13] Throughout the pore, the *o*-Ps atom is assumed to have a natural annihilation rate equal to λ_T plus an additional term. Below a critical radius R_a, this additional term is assumed to be the TE pick-off annihilation rate

$$\lambda_{Tokyo}(R) = \lambda_{TE}(R) + \lambda_T \qquad (R < R_a)$$

For $R \geq R_a$, the additional rate term is assumed to equal the TE pick-off rate for a pore of radius R_a, weighted by the probability of finding the *o*-Ps atom inside a sphere of radius R_a. The probability of finding the *o*-Ps atom *outside* a sphere of radius R_a is approximated by the fraction of pore radius greater than R_a raised to the power *b*, so the total annihilation rate is given by

$$\lambda_{Tokyo}(R) = \lambda_{TE}(R_a)\left[1 - \left(\frac{R - R_a}{R + \Delta R}\right)^b\right] + \lambda_T \qquad (R \geq R_a)$$

Being phenomenological in nature, this model must be fit to data in order to determine R_a and *b* and, thus, is heavily dependent upon the quality of the data used in the fit. It also has no explicit temperature dependence, and so it must be refit using data acquired in each temperature range of interest. This is a serious deficiency in predictive power because Ps lifetimes are observed to have very significant temperature dependence in porous media.[5,6,14]

IV. Rectangular Pore Extension of Tao−Eldrup

It is possible to extend the TE model, maintaining its simple physical foundations while avoiding calculational difficulties by switching from spherical to rectangular pore geometry.[15] The preliminary success of this approach has been demonstrated in previous publications.[5,6]

The detailed pore structure in porous films is in general unknown and is probably quite complicated. Pores can be interconnected,[5,7] or they can be isolated.[6,7] There is no compelling reason to choose spherical geometry over rectangular geometry. In such cases, cube side-length is as good a measure of physical pore dimensions as sphere diameter. In fact, it will be shown that the Ps lifetime is only modestly dependent upon the detailed pore geometry and is much more heavily dependent upon a geometry *independent* measure of pore size, the classical mean free path, $l = 4V/S$, where *V* and *S* are the volume and surface area of the pore. Indeed for very large pores, in which quantum mechanics can be neglected, the Ps lifetime does not depend on the specific pore geometry at all. It only depends on the number of times the Ps atom encounters a pore wall during its lifetime which is determined by the mean free path[16] and Ps velocity.

To calculate the expected lifetime of *o*-Ps in rectangular pores, the *o*-Ps wave functions are calculated as eigenstates of the *x*, *y*, and *z* momentum. In this basis, the solutions to the Schröedinger equation for a particle of mass *2m* (*m* being the electron mass) in an infinite rectangular well of side length *a*, *b*, and *c* in the *x*, *y*, and *z* directions are given by

$$\psi_{ijk} = \phi_i(x)\phi_j(y)\phi_k(z)$$

where

$$\phi_i(x) = \sqrt{\frac{2}{a}}\sin\left(\frac{i\pi x}{a}\right), \quad \phi_j(x) = \sqrt{\frac{2}{b}}\sin\left(\frac{j\pi x}{b}\right),$$
$$\text{and } \phi_k(x) = \sqrt{\frac{2}{c}}\sin\left(\frac{k\pi x}{c}\right)$$

The energies of these states are given by

$$E_{ijk} = \beta\left(\frac{i^2}{a^2} + \frac{j^2}{b^2} + \frac{k^2}{c^2}\right)$$

where

$$\beta = h^2/16m = 0.188 \text{ eVnm}^2$$

In the central portion of the pore, the annihilation rate is assumed to be λ_T. Within a distance δ of the walls, the annihilation rate is assumed to be equal to the spin-averaged rate λ_A. For convenience, we write this annihilation rate as

$$\lambda(x,y,z) = \lambda_A - \Lambda(x,y,z)$$

where

$$\Lambda(x,y,z) = \begin{cases} \dfrac{\lambda_S - \lambda_T}{4} & \text{for } \delta \leq x \leq a - \delta,\ \delta \leq y \leq b - \delta,\ \delta \leq z \leq c - \delta \\ 0 & \text{otherwise} \end{cases}$$

The expectation value of the annihilation rate can be expressed as the trace of the density matrix times the annihilation rate matrix. If the *o*-Ps atom is assumed to be in thermal equilibrium with the pore, it will statistically sample all states with a probability governed by the Boltzmann equation. In this case, the nonzero elements of the density matrix are given by

$$\rho_{ijk,ijk} = \frac{\exp(-E_{ijk}/kT)}{\sum_{i,j,k=1}^{\infty} \exp(-E_{ijk}/kT)} = \frac{\exp\left[-\frac{\beta}{kT}\left(\frac{i^2}{a^2}+\frac{j^2}{b^2}+\frac{k^2}{c^2}\right)\right]}{\sum_{i,j,k=1}^{\infty} \exp\left[-\frac{\beta}{kT}\left(\frac{i^2}{a^2}+\frac{j^2}{b^2}+\frac{k^2}{c^2}\right)\right]}$$

Because the density matrix is assumed to be diagonal for a system in thermal equilibrium, it is only necessary to calculate the diagonal elements of the annihilation rate matrix

$$\lambda_{ijk,ijk} = \langle ijk|(\lambda_A - \Lambda(x,y,z))|ijk\rangle = \lambda_A - \frac{\lambda_S - \lambda_T}{4}\int_\delta^{a-\delta} dx \int_\delta^{b-\delta} dy \int_\delta^{c-\delta} dz\, \phi_i^2(x)\phi_j^2(y)\phi_k^2(z) = \lambda_A - \frac{\lambda_S - \lambda_T}{4} G_i(a,\delta)G_j(b,\delta)G_k(c,\delta)$$

where

$$G_n(x,\delta) = 1 - \frac{2\delta}{x} + \frac{1}{n\pi}\sin\left(\frac{2n\pi\delta}{x}\right)$$

The expectation value of the annihilation rate in this rectangular extension to the Tao−Eldrup model (the RTE model), $\lambda_{RTE} = Tr\{\rho\lambda\}$, is then given by

$$\lambda_{RTE}(a,b,c,T) = \sum_{i,j,k=1}^{\infty} \rho_{ijk,ijk}\lambda_{ijk,ijk} = \lambda_A - \frac{\lambda_S - \lambda_T}{4} F(a,\delta,T)F(b,\delta,T)F(c,\delta,T)$$

where

$$F(x,\delta,T) = \frac{\sum_{i=1}^{\infty} G_i(x,\delta)\exp(-\beta i^2/x^2 kT)}{\sum_{i=1}^{\infty}\exp(-\beta i^2/x^2 kT)} = 1 - \frac{2\delta}{x} + \frac{\sum_{i=1}^{\infty}\frac{1}{i\pi}\sin\left(\frac{2i\pi\delta}{x}\right)\exp(-\beta i^2/x^2 kT)}{\sum_{i=1}^{\infty}\exp(-\beta i^2/x^2 kT)}$$

Because the density matrix is diagonal, this approach is equivalent to weighting the annihilation rates in each region of the pore with the square of the wave functions and then averaging together the annihilation rates for the excited states using a Boltzmann population distribution. The three limiting cases of thin one-dimensional (1D) sheetlike pores, square infinitely long two-dimensional (2D) channel-like pores, and compact three-dimensional (3D) cubic pores are easily modeled by setting one or more of the $F(x,\delta,T)$ equal to unity. There is one free parameter, δ, which is analogous to ΔR in the TE model. Unlike the spherical models above, the RTE pore dimensions extend to the hard walls of the well and are analogous to $R + \Delta R$, not R. Cube width, a, and pore radius, $R + \Delta R$, can be related by equating their mean free paths in which case $a = 2(R + \Delta R)$. To determine δ, the cubic RTE model is expressed as a function of effective pore radius by replacing cube width a with $2(R + \Delta R)$ and δ is chosen so that, at $T = 0$ K, $\lambda_{RTE}(R,0)$ closely agrees with $\lambda_{TE}(R)$ in the regime for which it is known to be accurate ($R < 1$ nm). Using this method, δ in the RTE model is determined to be 0.18 nm (see also ref 17, where a value of 0.19 is determined in this small-R regime). The material dependence of δ has not yet been sufficiently explored; however, the RTE model seems to acceptably fit pores in a variety of materials as will be demonstrated below.

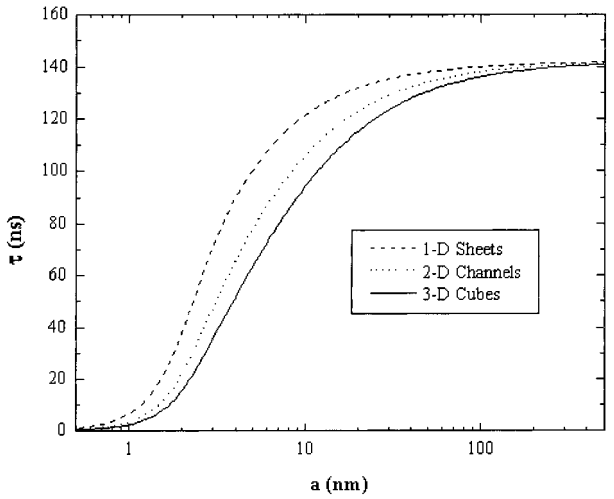

Figure 1. Ps lifetimes calculated with the RTE model vs pore size for three pore dimensionalities.

Figure 1 shows the RTE model for 1D sheets, 2D square channels, and 3D cubic pores. The calculated Ps lifetime is plotted as a function of the physical pore dimension (sheet spacing, channel width, and cube side-length). As is evident, there is a dependence on the dimensionality of the pores. All three curves have similar shape but are displaced laterally with respect to each other (corresponding to a multiplicative scale factor in pore length a). In the large pore (classical) regime, this is understood to be due to the fact that the Ps *mean free path* between wall collisions is different for each of the three dimensionalities considered.

To demonstrate the relatively weak dependence on detailed pore geometry, these three curves are replotted in Figure 2 as a function of the mean free path, $l_{1D} = 2a$, $l_{2D} = a$, and $l_{3D} = (2/3)a$. From a comparison of Figures 1 and 2, it is evident that, at least for channels and cubes, the lifetime is primarily dependent on the mean free path in the pore and only modestly dependent upon the detailed pore geometry. Although the curves in Figure 1 diverge over the range of 1−100 nm when plotted as a function of pore dimension, this range is reduced to 1−10 nm in Figure 2 when plotted as a function of the mean free path, l. The 2D channels and 3D cubes are very similar over almost the entire range of l. This indicates that the mean free

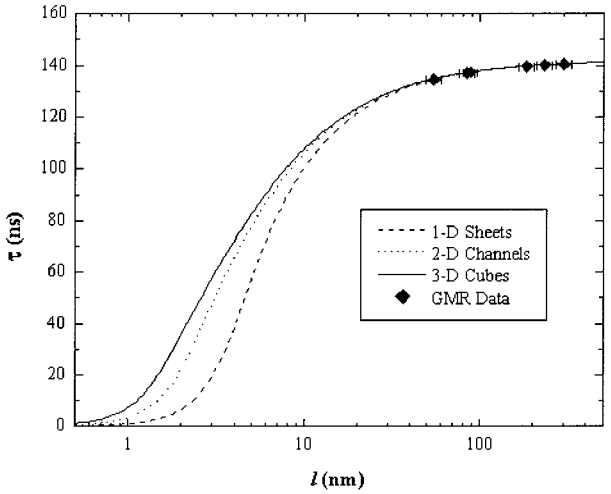

Figure 2. RTE model Ps lifetime vs mean free path, *l*, for three pore dimensionalities. Note that *l* is nominally a geometry independent measure of pore size, particularly for large pores.

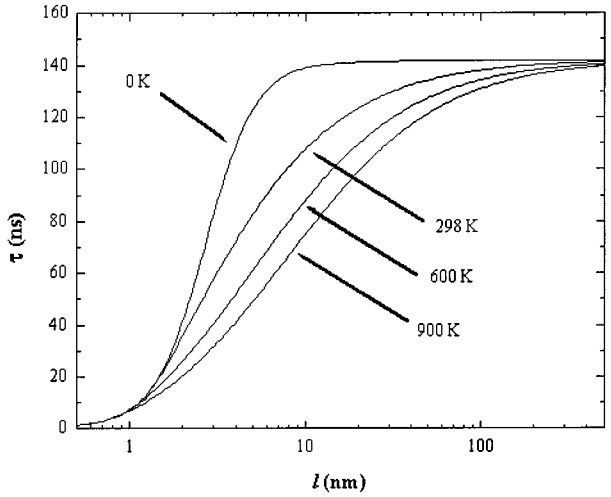

Figure 3. Temperature dependence of the Ps lifetime for cubical pores in the RTE calculation. The mean free path, *l*, is related to the cube side length by $l = {}^{2}/_{3}$a.

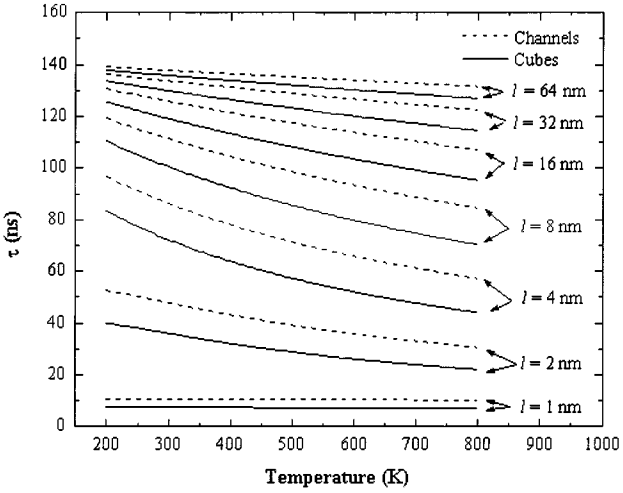

Figure 4. Ps lifetime vs temperature for a variety of mean free paths using both 2D and 3D pores in the calculation.

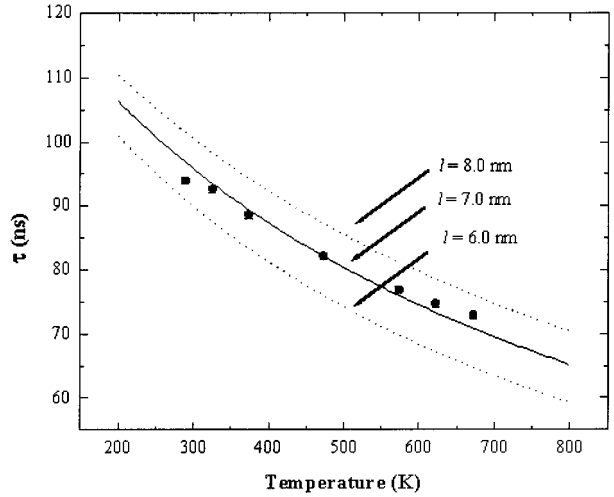

Figure 5. Ps lifetimes measured in a low-K porous silica film (Nanoglass A10B) as a function of film temperature and RTE curves (from ref 5).

path is the preferred linear measure of pore size to extract when using PALS (this is rigorously true for large pore dimensions). If detailed knowledge exists as to the physical pore geometry, the mean free path can easily be converted into a physical pore dimension. Also plotted in Figure 2 is high precision data collected in high porosity (>95%) silica powders referred to as GMR data.[16] It should be noted that the single fitting parameter δ was chosen so the RTE model agrees with the TE model in the subnanometer regime. Even though the model was calibrated in the quantum mechanical regime, the curves accurately account for data points in the classical regime 3 orders of magnitude larger in size, demonstrating the potentially broad applicability of this model.

An important feature of any excited-state extension of the TE model is that it should have *explicit temperature dependence*. Figure 3 shows RTE curves for several temperatures. Only cubic pore calculations are shown for clarity, and *l* is determined from the cube side-length. Recall that the RTE model was fit so that at $T = 0$ K it agrees with the TE model in the subnanometer regime. In fact, if the TE model is only modified to include the finite 142 ns *o*-Ps lifetime in the central portion of the pores, the TE curve and the RTE $T = 0$ K curve agree over the entire size range. That is equivalent to saying that the TE model involves only the ground state in the well/cavity.

Figure 4 shows the calculated temperature dependence of the Ps lifetime for a variety of pore sizes measured in terms of *l*. Both the 2D channel and 3D cubic versions are shown. As expected from the TE model, there is no significant temperature dependence for small pores. As can also be seen in the figure, for any given temperature, the 2D and 3D curves agree quite well for small pores and large pores; however, there is a slight dependence on pore geometry for intermediate sized pores. The dependence becomes more pronounced at higher temperatures (note that the logarithmic choice of pore size curves overemphasizes the discrepancy).

The expected temperature dependence can be exploited to systematically check the determination of pore size by collecting data at a variety of temperatures. Figure 5 shows lifetime data collected in a porous silica film[5] at various temperatures and, also, three RTE (cubic) temperature curves are plotted for comparison. These and other porous silica films we have studied typically have highly interconnected pores (rather than a distribution of closed pores, see ref 6) and thus display a single Ps lifetime corresponding to the *average* mean free path of Ps interacting with the total void volume. This lifetime spectrum is fitted beginning at 50 ns after Ps formation to ensure that Ps

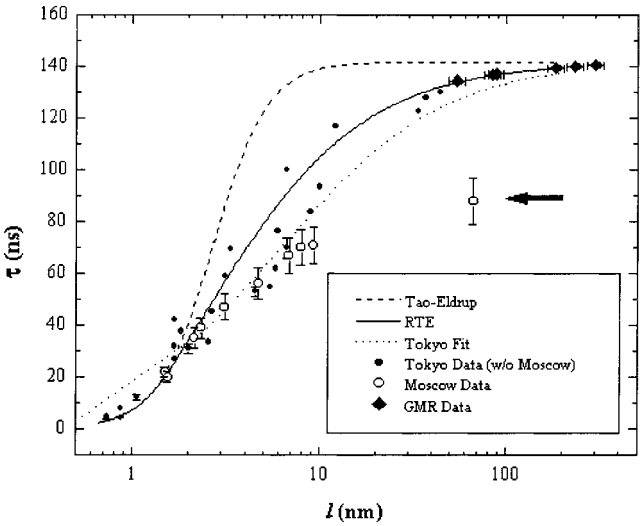

Figure 6. A comparison of the TE (ground state only) model, the Tokyo fit, and the RTE model with experimental data. The outlying Moscow point indicated by the arrow, which is anomalously low because of Ps lifetime quenching in air, was not used in the Tokyo fit. Unfortunately, the rest of the Moscow data were also collected in air and require correction.

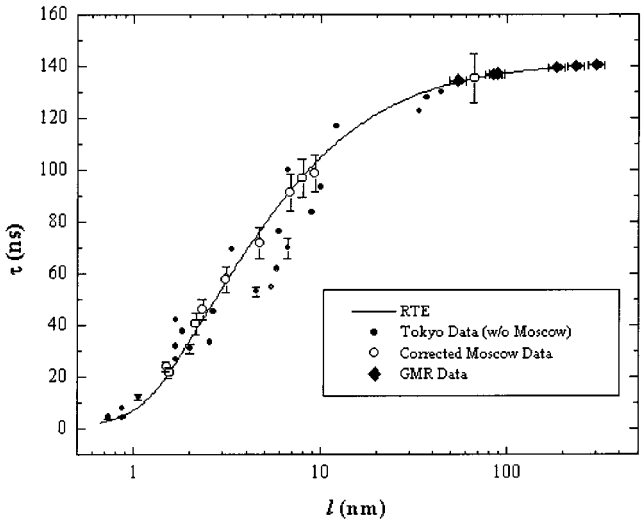

Figure 7. A comparison of the RTE model with experimental data, some of which (open circles) has been corrected for Ps quenching in air-filled silica gel. All of the experimental results are acquired in bulk silica gels.

has reached thermal equilibrium. As can be seen, the solid $l = 7.0$ nm curve fits the data quite well. The two dotted curves are plotted to demonstrate the sensitivity of the technique. Similarly good fits are also obtained using 2D channels for the pore model. Other temperature-dependent results have been observed,[6,14] and they appear to be in agreement with the RTE predictions.

Although the RTE model agrees with data in both the TE (subnanometer) and classical large-pore regimes, it is important to test its validity in the intermediate, semiclassical pore-size regime. In fitting their phenomenological model, the Tokyo group utilized data from the literature taken over a wide range of size scales, and it is interesting to compare the RTE model with these data and the Tokyo model.[13]

V. Comparison of the RTE and Tokyo Models

The data used by the Tokyo group are from nine separate studies of *o*-Ps lifetimes mostly in silica gels and zeolites ranging from 1970 to 1999[18−26] The pores are assumed to be spherical and in most cases it cannot be determined how the pore radii were calibrated. Uncertainty about pore dimensionality and inconsistent calibration of the pore sizes may explain the rather large spread in the data.

Figure 6 shows the TE model, the Tokyo fit, the cubic RTE model, and three sets of data. All of the data used in the Tokyo fit, except the data found in ref 27 of the Tokyo paper, are plotted as solid circles and are referred to collectively as the Tokyo data.[18−23,25,26] The data from ref 27 of the Tokyo paper and one additional data point from that reference (indicated by the arrow), are plotted as open circles and are referred to as the Moscow data.[24] The precision data collected in silica powders from Figure 2 are plotted as solid diamonds and are referred to as the GMR data.[16] This set was not used in the Tokyo fit. The curves and the data have been plotted as a function of mean free path, *l*, as opposed to pore radius.

Note that beyond $l = 2$ nm the data lie well below the TE model. This is direct evidence of its failure to accurately relate the *o*-Ps lifetime to pore size in larger pores. Also note that the large-pore Moscow data lie well below the RTE curve. Because the Tokyo curve includes fitting of these data, it is not surprising that the Tokyo fit also lies below the RTE curve. One troubling aspect of Figure 6 is that the Tokyo fit misses a significant portion of the precision GMR data for which the vertical error bars are much smaller than the plotting symbol. The problem is that the Moscow data were mainly collected in silica gels *while exposed to air*.[24] All of the open-circle data shown in Figure 6 were collected in air. The apparently specious point (indicated with an arrow) was not used in the Tokyo fit. Because air is known to quench Ps and significantly shorten its lifetime, it is not surprising that all of the Moscow data are systematically lower than the other data. The effect of quenching in air is to add an additional term to the annihilation rate that is comparable in magnitude to the vacuum decay rate. Thus, the very low lifetime of the outlying point is better thought of as a measure of the quenching effect of air. The magnitude of the quenching term can be estimated by determining the necessary annihilation rate to subtract from the unused Moscow datum point to bring it into agreement with the GMR data. This is determined to be 0.0040 ns^{-1} and can be subtracted from the rest of the Moscow data to correct for air quenching.

Figure 7 is a plot of the corrected Moscow data, the Tokyo data, the GMR data, and the cubic RTE model. Note that after correction, all of the Moscow data lie on the RTE curve even though it was normalized only at the one high-*l* point. The RTE curve is now in generally good agreement with all of the data.

VI. Comparison with Other Techniques

The agreement of the RTE model with zeolite, zirconia, and bulk silica gel data in Figure 7 is encouraging. There is still significant scatter in the experimental data, and this is probably the result of inconsistencies that arise when compiling data acquired in many laboratories over some two decades. There is certainly need to perform new calibration checks with particular focus on searching for material dependence in candidate thin film dielectrics. The main problem encountered is then simply stated: *there is no standard of pore size calibration for submicron thin films.* At this point, we can only compare results from independent methods and search for consistency. Such comparisons are well underway. Recently, identical porous silica films (Honeywell Nanoglass A10B) were studied by small angle neutron scattering (SANS)[27] and by beam-PALS[5] and the

deduced average chord/mean free path was 6.5 ± 0.1 and 7.5 ± 0.3 nm, respectively. Similarly, for Nanoglass A10C, the SANS[2] and PALS results are 5.8 ± 0.1 and 6.9 ± 0.3 nm. Close agreement between PALS and SANS at the 15 nm size scale in porous poly(arylene ether) films (Velox, supplied by Air Products and Chemicals Inc.) will soon be reported. In addition, the RTE model has been used to extract the diameter of tubular pores in two templated, silica-based low-*K* films supplied to us by Air Products and Chemicals Incorporated. A full 2D analysis was performed using infinitely long square channels in the RTE calculations and then converting channel width to tube diameter by equating mean-free paths. Our beam-PALS results using RTE analysis were compared to those from surface acoustic wave/gas absorption (SAW-BET) analysis, and good agreement was obtained: 2.8 vs 3.3 nm and 3.5 vs 3.7 nm, respectively. These isolated comparisons suggest that our extension of the TE model is valid and accurate for a range of materials. A systematic round robin comparison of a variety of low-*K* sample films is presently underway with NIST and IMEC to compare the results of PALS, SANS, and ellipsometric porosimetry (EP).[28] In the first round of several planned comparisons, highly consistent pore diameters were obtained[29] for a set of four porous methyl-silsesquioxane films (supplied by CCIC) spanning a diameter range of 3−8 nm. We are not aware of any inconsistencies with the RTE model at this time.

The complementary nature of the various characterization techniques has also been demonstrated. For example, PALS has been shown to be sensitive to pores much smaller than those observable with SANS and to closed porosity that is inaccessible to gas-absorption techniques. On the other hand, PALS too has some limitations. In order for PALS to be a useful probe of low-*K* materials, two conditions must be met. First, Ps must be able to form in the material. Although rare, in some materials (polyimides for example), Ps formation is suppressed because of an abundance of free radicals that scavenge electrons during the Ps formation process. The second condition is that Ps formed in the film must be able to diffuse into the porosity (otherwise PALS will probe the micropores of the molecular structure in the underlying bulk material instead of the mesopores of interest in low-*K* research). Indeed, in some large pore, low porosity films, SANS has demonstrated sensitivity to such large, isolated pores that are too disperse to be populated by Ps before its annihilation in the solid part of the material. Finally, we note that if the porosity is highly interconnected the film must be capped with a barrier layer in order to keep Ps from escaping into the vacuum system (escape leads to a systematically shortened film Ps lifetime coincident with the appearance of a 142 ns vacuum lifetime component). This effect has been observed in virtually every type of porous silica film. In most cases, these conditions do not pose a significant obstacle to the use of PALS as a probe of low-*K* materials. Indeed, the great strength of PALS may lie in its sensitivity to small pores, both isolated and interconnected, even if they are hidden beneath a diffusion barrier layer.

VII. Conclusion

The RTE model of Ps lifetime has been shown to be a highly successful and predictive model. It is firmly rooted in a fundamental physical model of Ps trapped in a quantum well. Once it is forced to agree with zeolite data and the TE model in the subnanometer regime, fixing its one free parameter, the model nicely agrees with data ranging up to 100 nm, over 3 orders of magnitude larger in size. The unphysical nature of the assumed rectangular pore shape is rendered unimportant once pore size is determined in terms of the mean free path. The RTE model, as a straightforward extension of the TE model, accounts for pores of *any size at any sample temperature*. Using this model, beam-PALS has been compared with other techniques in the characterization of pores in low-*K* dielectric films and is found to be highly consistent.

Acknowledgment. We would like to thank Todd Ryan, Wen li-Wu, Eric Lin, Mark O'Neil, Jim MacDougall, Simon Lin, and Jeff Wetzel for helpful discussions. This research is supported by the low-*K* Dielectric Program at SEMATECH and the National Science Foundation under Grants ECS-9732804 and PHY-9731861.

References and Notes

(1) See, for example, Jin, C.; Luttmer, J. D.; Smith, D. W.; Ramos, T. A. *MRS Bull.* **1997**, 39.
(2) Ryan, E.; Ho, H.; Wu, W.; Gidley, D.; Ho, P.; Drage, J. *IEEE Electron Devices*; *Proc. Int. Interconnect. Technol. Confer.* **1999**, *295*, 187.
(3) DeMaggio, G. B.; Frieze, W. E.; Gidley, D. W.; Zhu, M.; Hristov, H. A.; Yee, A. F. *Phys. Rev. Lett.* **1997**, *78*, 1524.
(4) Xie, L.; DeMaggio, G. B.; Frieze, W. E.; DeVries, J.; Gidley, D. W.; Hristov, H. A.; Yee, A. F. *Phys. Rev. Lett.* **1995**, *74*, 4947.
(5) Gidley, D. W.; Frieze, W. E.; Dull, T. L.; Yee, A. F.; Ryan, E. T.; Ho, H.-M. *Phys. Rev. B* **1999**, *60*, R5157.
(6) Gidley, D. W.; Frieze, W. E.; Dull, T. L.; Sun, J.; Yee, A. F.; Nguyen, C. V.; Yoon, D. Y. *Appl. Phys. Lett.* **2000**, *76*, 1282.
(7) Petkov, M.; Weber, M.; Lynn, K.; Rodbell, K. *J. Appl. Phys.* **2000**, *77*, 2470.
(8) Tao, S. J. *J. Chem. Phys.* **1972**, *56*, 5499.
(9) Eldrup, M.; Lightbody, D.; Sherwood, J. N. *Chem. Phys.* **1982**, *63*, 51.
(10) Wang, Y. Y.; Nakanishi, Y.; Jean, Y. C.; Sandrecski, T. C. *J. Polym. Sci., Part B: Polym. Phys.* **1990**, *28*, 1431.
(11) Cheng, K. L.; Jean, Y. C. *Positron and Positronium Chemistry*; Shrader, D. M., Jean, Y. C., Eds.; Elsevier: Amsterdam, The Netherlands, 1979; p 282.
(12) Goworek, T.; Ciesielski, K.; Jasinska, B.; Wawryszczuk, J. *Chem. Phys.* **1998**, *230*, 305 and references therein.
(13) Ito, K.; Nakanishi, H.; Ujihira, Y. *J. Phys. Chem. B.* **1999**, *103*, 4555.
(14) Goworek, T.; Ciesielski, K.; Jasinska, B.; Wawryszczuk, J. *Radiat. Phys. Chem.* **2000**, *58*, 719.
(15) Jasinska, B.; Koziol, A. E.; Goworek, T. *J. Radioanal. Nucl. Chem.* **1996**, *210*, 617.
(16) Gidley, D. W.; Marko, K. A.; Rich, A. *Phys. Rev. Lett.* **1976**, *36*, 395. Gidley, D. W. Ph.D. Thesis, The University of Michigan, 1979.
(17) Ciesielski, K.; Dawidowicz, A. L.; Goworek, T.; Jasinska, B.; Wawryszczuk, J. *Chem. Phys. Lett.* **1998**, *289*, 41.
(18) Nakanishi, H.; Ujihira, Y. *J. Phys. Chem.* **1982**, *86*, 4446.
(19) Ito, Y.; Yamashina, T.; Nagasaka, M. *Appl. Phys.* **1975**, *6*, 323.
(20) Chuang, S. Y.; Tao, S. J. *Can. J. Phys.* **1973**, *51*, 820.
(21) Ito, K.; Yagi, Y.; Hirano, S.; Miyayama, M.; Kudo, T.; Kishimoto, A.; Ujihira, Y. *J. Ceram. Soc. Jpn.* **1999**, *107*, 123.
(22) Goldanskii, V. I.; Levin, B. M.; Mokrushin, A. D.; Kaliko, M.; Pervushina, M. N. *Dokl. Adad. Nauk SSSR* **1970**, *191*, 855.
(23) Chuang, S. Y.; Tao, S. J. *J. Chem. Phys.* **1970**, *52*, 749.
(24) Mikrushin, A. D.; Levin, B. M.; Goldanskii, V. I.; Tsyganov, A. D.; Bardyshev, I. I. *Russ. J. Phys. Chem.* **1972**, *46*, 368.
(25) Goldanskii, V. I.; Mokrushin, A. D.; Tatur, A. O.; Shantarovich, V. P. *Appl. Phys.* **1975**, *5*, 379.
(26) Hopkins, B.; Zerda, T. W. *Phys. Rev. Lett* **1990**, *145*, 141.
(27) Wu, W. L.; Wallace, W. E.; Lin, E. K.; Lynn, G. W.; Glinka, C. J.; Ryan, E. T.; Ho, H.-M. *J. Appl. Phys.* **2000**, *87*, 1193.
(28) Mogilnikov, K. P.; Polovinkin, V. G.; Dultsev, F. N.; Baklanov, M. R. *Mater. Res. Soc. Symp. Proc.* **1999**, *565*, 81.
(29) Kondoh, E.; Baklanov, M.; Lin, E.; Gidley, D.; Nakashima, A. *Jpn. J. Appl. Phys.* **2001**, *40*, L323.